S-CUBED

A Division of Maxwell Laboratories, Inc.

UCRL--15860-Vol.2

DE87 006684

CONTAMINANT TRANSPORT DURING ATMOSPHERIC PUMPING OF A NUCLEAR CHIMNEY

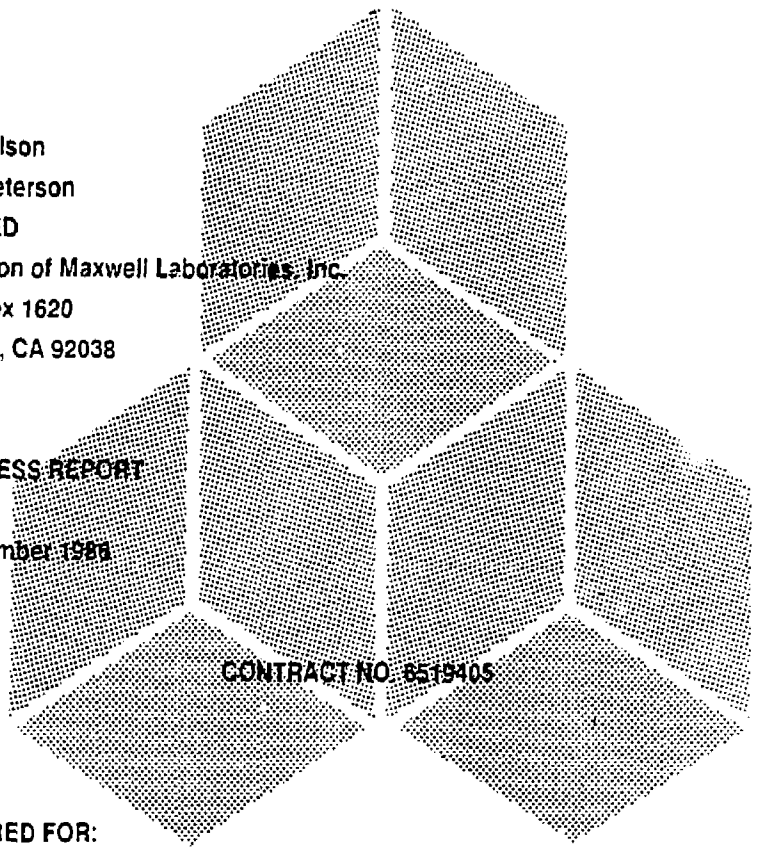

R. H. Nilson
E. W. Peterson
S-CUBED
A Division of Maxwell Laboratories, Inc.
P. O. Box 1620
La Jolla, CA 92038

PROGRESS REPORT

1 September 1986

CONTRACT NO. 6519405

PREPARED FOR:

LAWRENCE LIVERMORE NATIONAL LABORATORY
P. O. BOX 5012
LIVERMORE, CA 94550

P. O. Box 1620, La Jolla, California 92038-1620
(619) 453-0060

SSS-R-86-7726

CONTAMINANT TRANSPORT DURING ATMOSPHERIC PUMPING OF A NUCLEAR CHIMNEY

R. H. Nilson
E. W. Peterson
S-CUBED
A Division of Maxwell Laboratories, Inc.
P O Box 1620
La Jolla, CA 92038

ABSTRACT

Cyclical variations in barometric pressure cause an oscillatory up-and-down motion of gases within the chimney produced by an underground nuclear test. Analytical and experimental modeling of this atmospheric pumping mechanism has been undertaken to better understand and to quantify the associated rates of cavity gas migration toward the earth's surface and the probable rate of release to the atmosphere. Three different types of models are being investigated.

- Homogeneous porous medium
- Fractured medium with impermeable matrix blocks
- Double-porosity media consisting of fracture networks among porous matrix blocks.

A primary purpose of this work is to understand how the oscillatory character of the atmospheric pumping process might significantly enhance the contaminant transport in any or all of the three classes of media. One can easily imagine that a "ratchet mechanism" could carry contaminants to successively higher and higher elevations on the repeated upward phases of the motion. This sort of mechanism is known to be operative in homogeneous porous media at high frequencies. Such enhancement can probably occur in double-porosity media at much lower frequencies, because the matrix blocks provide a temporary storage location in which the contaminant might reside between upward cycles.

This preliminary report describes some of the analytical, numerical, and experimental work which have been completed. Significant progress has been made in several different areas:

- Identify physical mechanisms of importance.
- Formulate simple first-order models of these processes.
- Conduct laboratory experiments which demonstrate the mechanisms.
- Determine which material properties of the medium are critical.
- Develop numerical models of the important processes.

TABLE OF CONTENTS

LIST OF FIGURES

LIST OF FIGURES (Continued)

CONTAMINANT TRANSPORT DURING ATMOSPHERIC PUMPING OF A NUCLEAR CHIMNEY

1. INTRODUCTION

Cyclical variations in barometric pressure cause an oscillatory up-and-down motion of gases within the chimney produced by an underground nuclear test. Analytical and experimental modeling of this atmospheric pumping mechanism has been undertaken to better understand and to quantify the associated rates of cavity gas migration toward the earth's surface and the probable rate of release to the atmosphere. Three different types of models are being investigated.

- Homogeneous porous medium
- Fractured medium with impermeable matrix blocks
- Double-porosity media consisting of fracture networks among porous matrix blocks.

The first two models represent end-members in the spectrum of geologic media, while the last is a more realistic composite model which can simulate any of the intermediate behaviors as well as the end-members.

Computer modeling already undertaken reinforces the expectation that the cavity gas migration characteristics of a homogeneous porous media may be very different than those of fracture dominated media, even in circumstances where both have "equivalent" bulk flow characteristics, as inferred by comparing pressure variations within the chimney with those on the surface. The primary difference is that the fracture-dominated medium has a much smaller accessible porosity (i.e., capacitance) than the "equivalent" homogeneous porous medium, so there is a much smaller buffer volume between the chimney and the surface. The difference in radioactive gas transport is so great that the fractured medium may vent a significant amount of cavity gas during the first atmospheric low, whereas the homogeneous medium would

require tens or hundreds of cycles to pump the same amount of cavity gas to the surface. So, to distinguish between these black and white extremes, we are currently investigating the double-porosity model in which the accessible buffer volume lies somewhere between the extremes of the fracture porosity and the total porosity of fractures and matrix blocks.

Laboratory experiments are also being conducted to demonstrate some fundamental concepts, to verify the numerical modeling described above and, most importantly, to learn whether or not the oscillatory character of the atmospheric pumping process might significantly enhance the contaminant transport in any or all of the three classes of media. One can easily imagine that a "ratchet mechanism" could carry contaminants to successively higher and higher elevations on the repeated upward phases of the motion. This sort of mechanism is known to be operative in homogeneous porous media at high enough frequencies (about ~1 cps or greater). Such enhancement can probably occur in double-porosity media at much lower frequencies, because the matrix blocks provide a temporary storage location in which the contaminant might reside between upward cycles.

This preliminary report describes some of the analytical, numerical, and experimental work which have been completed. Significant progress has been made in several different areas.

- Identify physical mechanisms of importance
- Formulate simple first-order models of these processes
- Conduct laboratory experiments which demonstrate the mechanisms
- Determine which material properties of the medium are critical
- Develop numerical models of the important processes

We hope to continue to participate in this project over the next year, with a change of focus toward

- Numerical implementation of double-porosity models

- Comparison of calculational results with laboratory and field data

- Formulate and develop experimental techniques which provide property data relevant to the prediction of atmospheric pumping transport

The last consideration is particularly challenging, considering the nonhomogeneity of the medium at many different scales, the breadth and depth of the region of interest, and the alteration of the medium caused by the nuclear explosion and the cavity collapse.

2. ONE DIMENSIONAL TRANSPORT MODELS

To explore the influence of various transport properties on the migration of radioactive gases, let us first consider one-dimensional vertical transport in a homogeneous single-porosity medium. We will begin by examining the case of quasistatic gas motion in the absence of dispersion; this provides a simple estimate for the differential displacement, ΔL, of a contaminant during a cycle of atmospheric pumping. This limiting case applies to a medium with a very high diffusivity and a very small dispersivity. In reality, a smaller diffusivity will tend to inhibit the radioactive gas migration, but a larger dispersivity will tend to enhance the migration, as we shall see.

2.1 QUASISTATIC MODEL: THE ROLE OF POROSITY

The quasistatic displacement model is illustrated schematically in Figure 1 where a permeable layer of overall depth L is subjected to a surface pressure variation with a peak to peak amplitude of ΔP. The differential displacement ΔL of a gas particle or an interface (e.g., between contaminated versus non-contaminated gas) can be estimated from the formula

$$\frac{\Delta L}{L_o} = \frac{\Delta P}{P_o} \sim \frac{1}{30}$$

Figure 1

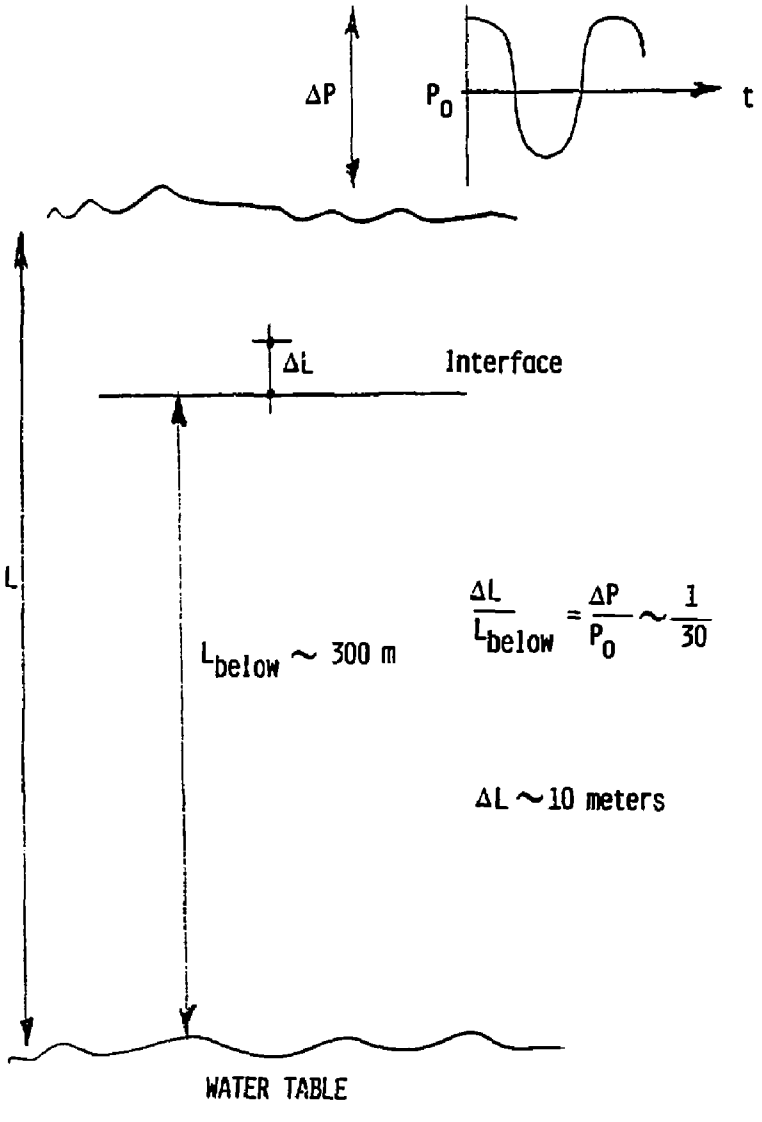

Figure 1. When diffusivity is large, upward displacements can be predicted by a simple quasi-steady approximation.

in which P_o is the ambient pressure level and L_o is the depth of gas beneath the interface. This formula is based on the observation that the volume of gas below the interface ($V_o = A_{cc}\,\phi L_o$) expands into an incremental volume of $\Delta V = A_{cc}\,\phi\Delta L$ during an isothermal pressure change in which $\Delta V/V_o = \Delta P/P_o$. Note that the porosity, ϕ, of the medium must be uniform in order that $\Delta L/L_o$ be identical to $\Delta V/V_o$. Also, there must be a lower boundary to the gas-filled porous layer, as imposed by either a water table or a low permeability bed rock.

For the typical example in Figure 1, a pressure variation of $\Delta P/P_o = 1/30$ produces a differential displacement of only $\Delta L = 10$ meters for an interface located 300 meters above the water table. Such a model might be applicable to a nuclear chimney which had collapsed all the way to the surface, leaving a column of relatively homogeneous rubble. If the porosity of the rubble tended to increase toward the surface, as expected, then the differential displacement would be even smaller than estimated above.

For the partially collapsed nuclear chimney shown in Figure 2, there is a large well-connected volume V_c which lies beneath a permeable column which has a uniform porosity, ϕ. Here, the quasistatic displacement of the cavity gas interface would be roughly given by

$$\Delta L = \frac{V_c}{A_{cc}\phi}\,\frac{\Delta P}{P_o}$$

For a cavity radius of 60 meters, the differential displacement would be only 30 meters for an overburden porosity of 10%. However, if the available porosity above the void were only 1%, the corresponding differential displacement of 300 meters is comparable to the burial depth and, hence, poses a containment threat.

The behavior of this quasistatic model is entirely controlled by the assumed geometry and, more specifically, the distribution of porosity within the system. The geometries in Figures 1 and 2 are essentially one dimensional. A more realistic two-dimensional treatment would permit the horizontal flow of gas

Figure 2

CHIMNEY MODEL

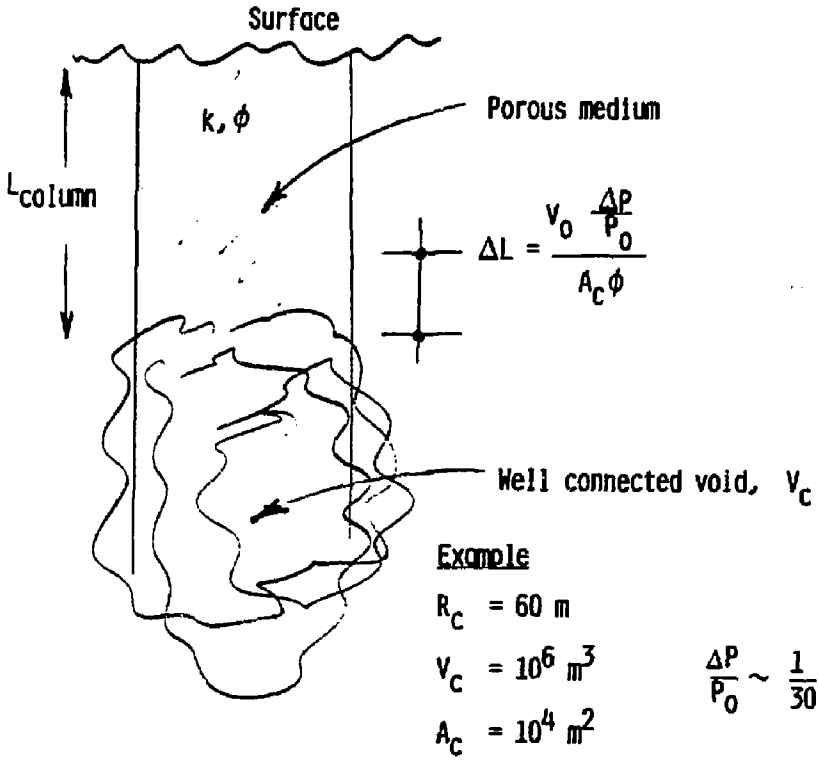

	Homogeneous	Intermediate	Fractured
ϕ	0.1	0.01	0.001
ΔL	30	300	3000

Figure 2. Upward displacements are largest when the accessible porosity, and hence the buffer volume of the overburden is small.

between the chimney and its surroundings. This could either aggravate or mitigate the vertical transport, depending upon the relative magnitude of transport properties of the chimney versus its surroundings.

The quasistatic model clearly illustrates the importance of overburden porosity in reducing the threat of radioactive gas migration. In essence, the overburden porosity provides a buffer volume between the cavity gas and the surface. During atmospheric lows, the cavity gas expands upward into this buffer volume. During atmospheric highs, the process is reversed. Stated most simplistically, if the volume of contaminated gas is V_o, and the fractional pressure change is 1/30, then a buffer volume of $V_o/30$ is required to prevent surface venting. It is emphasized that the capacitance effect of the buffer volume is achieved by displacement, not by pressurization; the contaminated gas flows upward into the bottom of the buffer as the fresh gas flows out the top.

The two principle simplifications of this model are its quasistatic nature, since pressure is assumed uniform everywhere within the medium, and its homogeneity which allows the interface to move up and down without dispersion. The quasistatic supposition tends to conservatively overestimate the extent of gas migration, whereas the absence of dispersion tends to underestimate the vertical transport of contaminant, as explained further below.

2.2 DYNAMIC MODEL: THE ROLE OF DIFFUSIVITY

The quasistatic analysis of the preceding section assumes that the gas pressure is, at any instant, uniform throughout the permeable medium. The pressure at every depth was assumed to adjust instantaneously to changes in the surface pressure. This ignores the fact that such pressure changes can occur only as a result of gas flow and, hence, there is always a finite time lag and an attenuation in amplitude which is associated with the process of pore fluid "diffusion".

The dynamics of a one-dimensional gas flow in a permeable medium can be described by a relatively simple set of equations. Conservation of mass requires that

$$\phi \frac{\partial \rho}{\partial t} + \frac{\partial}{\partial x} (\rho u) = 0$$

in which ϕ is porosity, u is the superficial velocity of the gas, and ρ is the gas density. For the moderate gas velocities which are induced by atmospheric pumping, the balance between pressure forces and viscous forces can be described by Darcy's law

$$u = - \frac{k}{\mu} \frac{\partial P}{\partial x}$$

in which k is the formation permeability, ϕ is the gas pressure, and μ is the gas viscosity. If it is further assumed that the pumping process is nearly isothermal (T = constant), that the gas is ideal (ρ = P/RT), and that the changes in gas density are relatively small ($\Delta\rho/\rho_o = \Delta P/P_o << 1$), then the transport equations can be combined to obtain the following diffusion-like equation for the gas pressure.

$$\frac{\partial P}{\partial t} = \alpha \frac{\partial^2 P}{\partial x^2} \quad : \quad \alpha = \frac{kP_o}{\mu\phi}$$

in which α is the so-called pore fluid diffusivity. This equation can be readily solved by numerical methods for any prescription of the surface pressure variation as a function of time.

The influence of the pore fluid diffusivity is illustrated in Figure 3 where the prescribed pressure variation at the top of a 300 meter porous column is the sine wave labeled P_{top}, having an amplitude of 1/30 atmosphere and a period of 100 hours, typical of an atmospheric pumping process. If the diffusivity of the porous column is very large, the bottom of the column is in good communication with the top, and the bottom pressure closely tracks the top pressure, as in the calculation with $\alpha = 10^5$ m^2/hr. corresponding to a permeability of 300 Darcies and a porosity of 10%. However, if the diffusivity is relatively small, the bottom is hardly aware of the pressure changes which occur at the top, as in the calculation with $\alpha = 10^3$ m^2/hr. corresponding to a permeability of 3 Darcies.

Figure 3

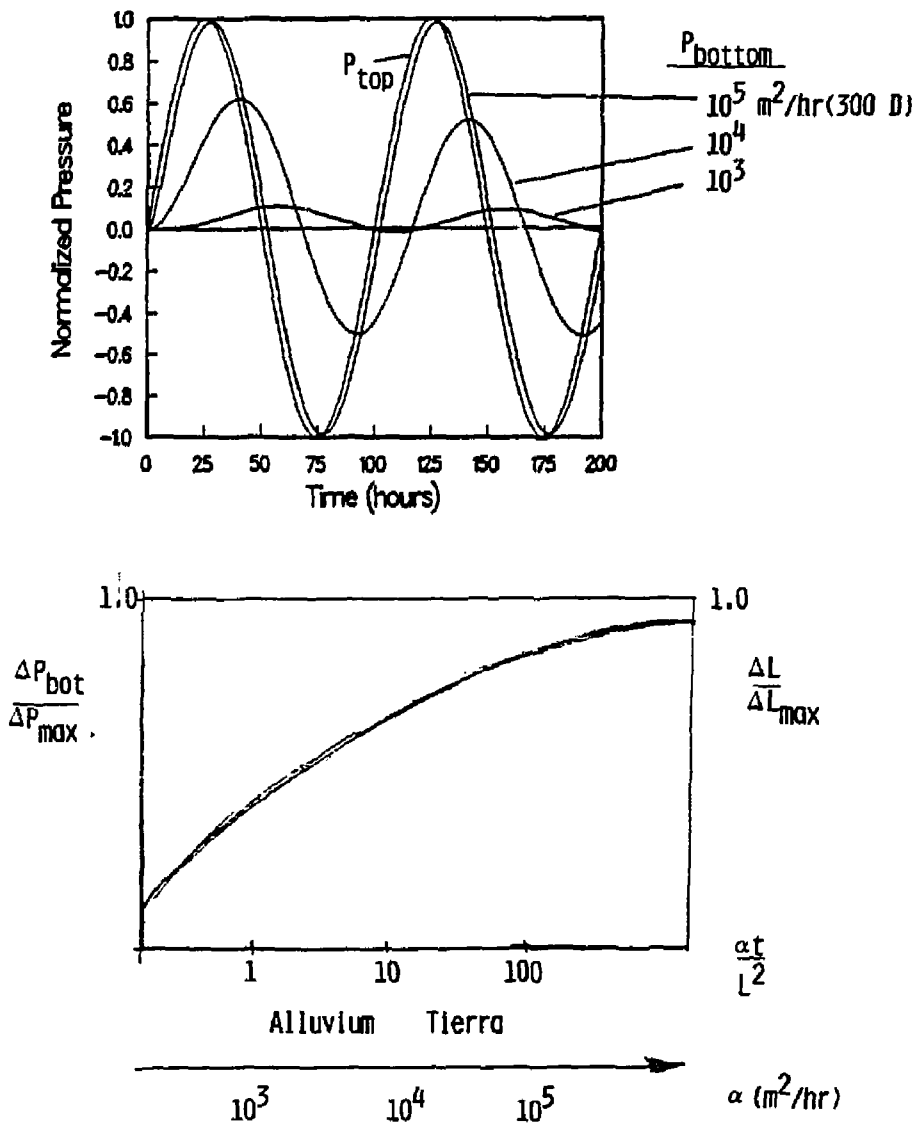

Figure 3. A small diffusivity (<10^4 m^2/hr) reduces the pressure changes in the cavity and reduces the upward displacement of contaminants.

The transit time for a pressure wave to traverse the permeable column is roughly $t = L^2/\alpha$, suggesting that the bottom pressure should closely track the top pressure whenever the period τ of the surface disturbance is considerably longer than the transit time of the wave. Thus, as indicated in the lower frame of Figure 3, the pressure should be relatively uniform through the column and the quasistatic displacement model should provide reasonable estimates whenever

$$\frac{\alpha\tau}{L^2} \gg 1$$

For our example problem with $L = 300$ meters and a porosity of $\phi = 0.1$, $\alpha\tau/L^2 > 1$ so long as the diffusivity is greater than 10^3 m^2/hr. If the diffusivity is much greater than this, as was measured for the Tierra site, then the time-lag effects associated with finite pore fluid diffusivity will not be helpful in mitigating the vertical transport of contaminated gases. In which case the quasisteady model becomes applicable and the outcome becomes independent of diffusivity. It should, however, be reemphasized that this insensitivity to diffusivity is critically dependent upon the existence of the lower boundary imposed by the water table or the paleozoic layers.

The diffusivity would always be a controlling consideration if the gas-filled porous domain were bottomless. The surface arrival of contaminant might then be crudely estimated as

$$t = \frac{\Delta L^2}{\alpha} \frac{P_o}{\Delta P}$$

if the contaminant were travelling upward from an initial depth, ΔL, below the surface due to a surface pressure depression of ΔP. The quantity $P_o/\Delta P$ appears here because the particle velocity induced by the pressure wave is only $\Delta P/P_o$ as large as the propagation velocity of the pore fluid diffusion wave. In a situation like Tierra with $\alpha \sim 10^5$ m^2/hr, a pressure wave could travel 300 meters in a time of $t = \Delta L^2/\alpha = 1$ hr, and the radioactive gas could traverse that same distance in about 30

hours for $\Delta P/P_o = 1/30$. However, this amount of upward gas displacement could only occur if the gas-filled porous region extended to a depth of $\Delta L\ P_o/\Delta P = 300 \times 30 = 10{,}000$ meters below the surface.

2.3 NONHOMOGENEITY AND MULTIDIMENSIONALITY: THE ROLE OF DISPERSIVITY

The one-dimensional modeling of the preceding sections assumes that all of the gas particles at any given elevation have identically the same vertical velocity. Thus, any interface between contaminated versus non-contaminated gas must necessarily move upward and downward in a piston-like fashion, without any dispersion of a sharp front. In reality, the gas will move faster and farther along preferential paths, such as fractures, than it does in the surrounding permeable matrix. Thus, nonhomogeneities can cause significant dispersion of the contaminant interface and greatly hasten the surface arrival of radioactive gases.

Even though the dispersive effects are generally multidimensional in origin, they are often modeled in a one-dimensional fashion by analogy with molecular diffusion. The one-dimensional equation for conservation of an inert chemical component travelling through a porous medium is

$$\frac{\partial C}{\partial t} + \frac{\partial}{\partial x}\left[\frac{u}{\phi} C\right] = \frac{\partial}{\partial x}\left[D \frac{\partial C}{\partial x}\right]$$

in which C is the concentration, u/ϕ is the interstitial velocity of the gas, and D is the dispersion coefficient which includes the effects of molecular diffusion as well as the mechanical dispersion caused by the multidimensionality of the flow

$$D = D_{molecular} + D_{mechanical}$$

Typically, the molecular diffusion coefficient for gases moving through air is of the order

$$D_{molecular} \sim 2 \times 10^{-5}\ m^2/s \sim 10^{-1}\ m^2/hr$$

and the mechanical dispersion coefficient is usually assumed to depend linearly on the interstitial velocity, u/ϕ, such that (for the high Peclet numbers of interest here)

$$D_{mechanical} \sim \frac{u}{\phi}\,\delta$$

which serves as a defining equation for the so-called dispersivity coefficient

$$\delta = \text{dispersivity}$$

Depending upon the degree of nonhomogeneity, the dispersivity can vary anywhere from a grain size on the order of 10^{-4} meters to a block size on the order of 10 meters.

The influence of dispersion is illustrated in Figure 4 which shows the vertical distribution of contaminant within the column at various instants in time for atmospheric pumping of a porous column. In the absence of dispersion, the contaminant interface moves upward by a maximum amount, $\Delta L/L \sim 1/5$, as indicated by the profile for $Dt/L^2 = 0$ in Figure 4. Successive cycles of pumping would simply reproduce this same profile at each atmospheric low. However, when a finite dispersion is included in the calculation, the interface will gradually spread out over time, reaching the top of the column in a time of roughly $t = L^2/D$.

The magnitude of the dispersion coefficient and the elapsed time for surface arrival of contaminant can be readily estimated from formulas already given. For a relatively high diffusivity, the differential displacement of the gas is on the order of $\Delta L \sim L_o\, \Delta P/P_o \sim 10$ meters, as discussed previously in Figure 2. If the period of oscillation is roughly $\tau = 100$ hrs, the gas velocity is about $u \sim \Delta L/\tau \sim 0.1$ m/hr. Finally, depending upon the degree of nonhomogeneity of the medium, the dispersivity might range from 0.1 m to 10.0 m, with the larger values probably most appropriate for fracture-dominated media having a relatively small fracture porosity. This range of parameters would suggest a dispersion coefficient in the range $D \sim 10^{-1} - 10^{3}$ m^2/hr, and a surface arrival time of $10 - 10^{5}$ hrs, as outlined in the table at the bottom of Figure 4. Thus, the estimated arrival time ranges from several hours to several years. So, there is certainly a need to tighten these

Figure 4

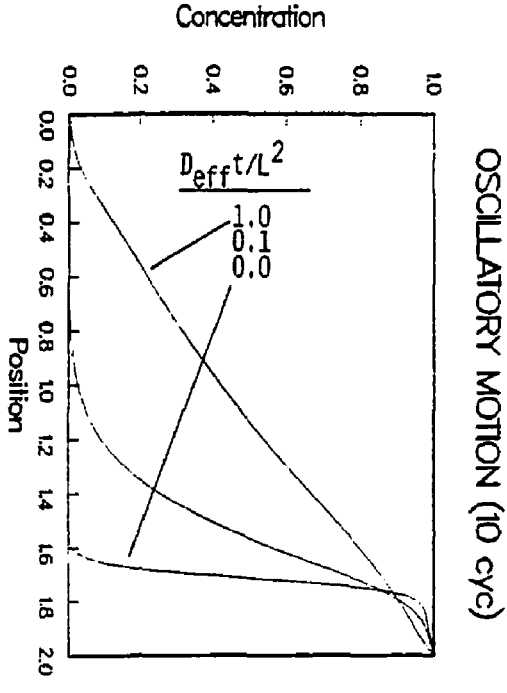

$$\frac{\partial C}{\partial t} \simeq \frac{D}{\phi} \frac{\partial^2 C}{\partial x^2}$$

$$D = u\delta$$

$$D_{eff} = \frac{u}{\phi}\delta$$

$$t_{arrival} = \frac{L^2}{D_{eff}}$$

$$u \sim \frac{\Delta L}{\tau} \sim \frac{10\ m}{100\ hr}$$

	Homogeneous	Intermediate	Fractured
ϕ	0.1	0.01	0.001
δ (m)	0.1	1.0	10.0
D (m^2/hr)	10	10^3	10^5
$t_{arrival}$ (hr)	10^5	10^3	10

Figure 4. Dispersion greatly enchances the upward transport in nonhomogeneous media, but it is difficult to estimate even the order of magnitude of the dispersivity.

estimates, either by direct field measurements or by establishing a connection between the dispersion mechanism and some other transport properties which can be measured in the field.

The primary physical mechanism of dispersion in unidirectional (i.e., non-oscillatory) flow is illustrated in Figure 5 for three different flow configurations. In a channel or a capillary tube, the centerline velocity is greater than the fluid velocity near the wall, so the contaminant travels fastest up the center. The advance of the salient is, however, constrained by the fact that molecular diffusion in the lateral direction depletes the concentration in the central finger of contaminant. An analogous effect occurs in a homogeneous porous medium due to the varying length (i.e., tortuosity) of adjacent stream tubes as well as varying velocity from one stream tube to the next. An extreme case occurs in fractured porous media which may be viewed as a composite of channels and porous matrix blocks. Both of the proceeding mechanisms are then operative in a simultaneous fashion, and it is obvious that the fluid travels much faster along the fractures than through the blocks.

The oscillatory flows of interest in atmospheric pumping are subject to all of the dispersion mechanisms noted previously for unidirectional flow. In addition, there are a number of "ratchet mechanisms" which should also enhance the vertical dispersion, as noted in Figure 6. In an oscillating channel flow, some of the contaminant which travels rapidly up the center (during an upstroke) diffuses into the slow-speed boundary layers along the wall, where it will not be swept all the way down again (during the next downstroke). If the wall of the channel is porous, as in a fractured permeable medium, this same sort of ratchet mechanism is further enhanced by two additional processes, since the contaminant can be carried into the porous walls of a fracture both by molecular diffusion and by Darcian seepage. Thus, the walls provide a temporary residence where the contaminant can "hide" between successive upward cycles of motion. Dogs are well aware of these enhancement mechanisms, which explains why they pant so fast when they are hot.

Figure 5

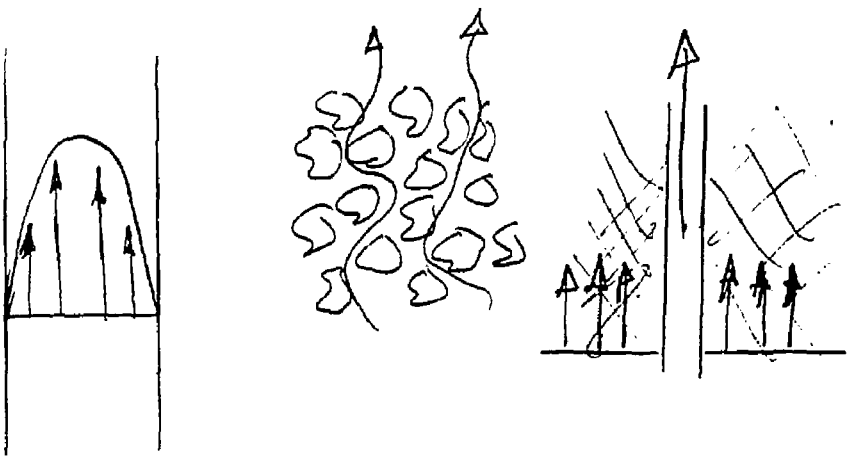

Figure 5. Nonuniformity of the fluid velocity causes dispersion of contaminants in channel flows, porous media and in fractured porous media, even in the absence of oscillatory motions.

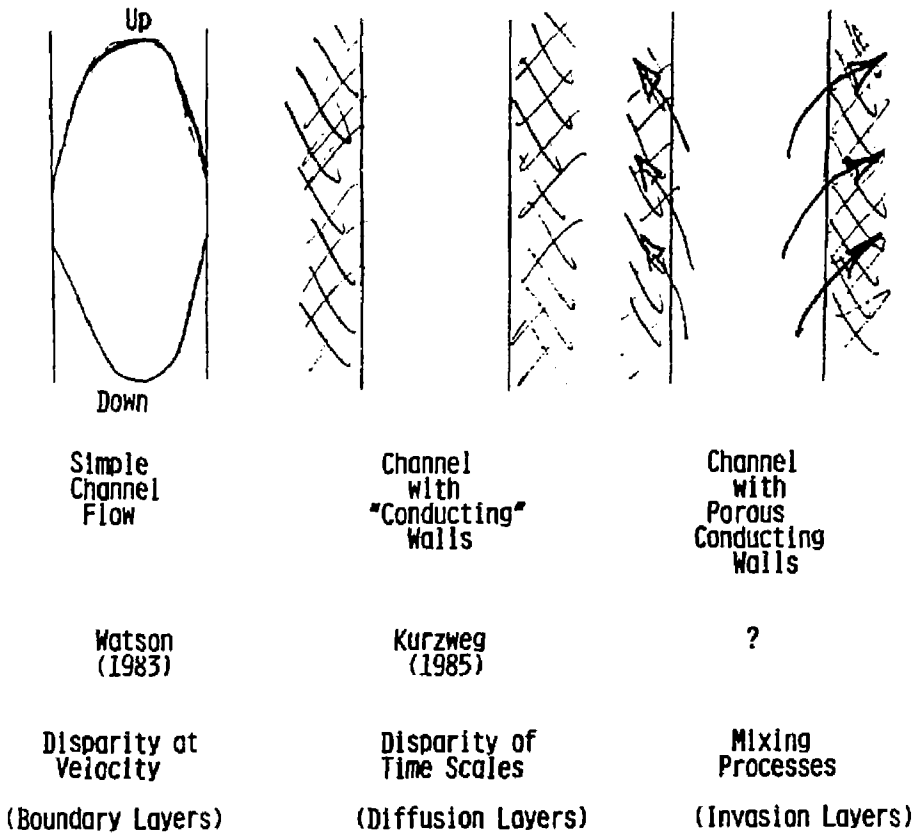

Figure 6. Oscillatory motions can enhance dispersion because of "ratchet" mechanisms which carry contaminant to higher and higher elevations at each successive upstroke of motion.

In the geologic media of interest, all of the mechanisms noted above will be further modified by the nonhomogeneous arrangement of fractures, their degree of connectivity, and their inclinations to the predominant pressure gradient, as illustrated schematically in Figure 7. Also, one might expect that the vertically layered structure of a geologic medium might be another important consideration in the dispersion process. Considering the overall complexity of this transport problem, there is a need for laboratory experiments which clarify the issues as well as field experiments which characterize the media of interest.

3. LABORATORY EXPERIMENTS

A series of laboratory experiments were undertaken to better understand the physical mechanisms which are important in the vertical transport of contaminated gases during atmospheric pumping. The initial scoping experiments described here provide some qualitative and quantitative information concerning the roles of molecular diffusion, mechanical dispersion, and pore fluid diffusivity, all of which were discussed in the preceding sections. In particular, it was found that the interaction between a simulated fracture and its permeable surroundings (i.e., the ratcheting mechanism illustrated on the right side of Figure 6) can significantly hasten the surface arrival of radioactive gases.

The experimental apparatus is illustrated schematically in Figure 8. The sample holder is a lucite tube 10 cm in diameter by 2 m long. The sample is constrained between perforated plates leaving plenum chambers at both ends. An oscillatory pressure variation can be produced within the upper plenum by the piston-like reciprocating motion of a well-sealed bellows device called a rolling diaphragm. At the onset of an experiment, a tracer gas is injected into the lower plenum to simulate the radioactive gas at the bottom of a nuclear chimney. During an experiment, gas samples are periodically extracted from the upper and lower plenums by insertion of a hypodermic needle through a septum seal. After each extraction of a sample, a compensating amount of clean air is reinjected to offset the slight pressure reduction caused by the extraction. A gas chromatograph is used to determine the concentration of tracer gas within each sample, providing a time history of the concentration in each plenum.

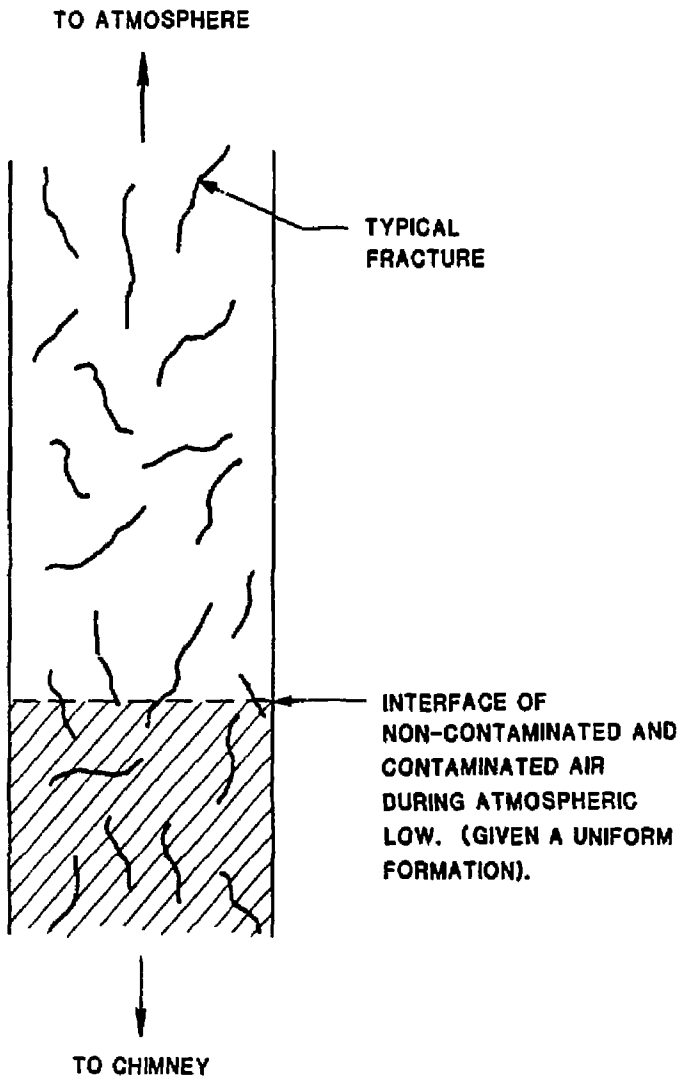

Figure 7. Nonuniformity of fracture orientation, relative to pressure gradient, causes irreversibilities during upward and downward phases of flow.

Figure 8

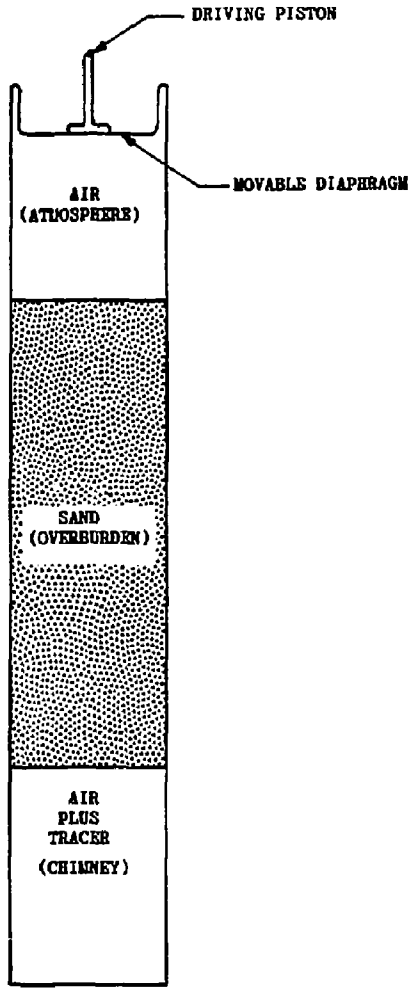

Figure 8. Experimental apparatus induces an oscillatory motion by reciprocating motion of a piston.

Typical pressure histories at the top and bottom of the column are shown in Figure 9. The peak to peak pressure variation is on the order of 0.4 psi, comparable to the atmospheric pumping process of interest. The period of the pressure oscillation is, however, much shorter in the laboratory (~1 min) than in the field (~100 hr), to provide many cycles of oscillation in a short time and, also, to compensate for the shorter length scale used in the laboratory. (A scaling or similitude analysis was used in designing the experiment but will not be described in detail in this preliminary report.) The experiment was designed such that the pressure at the bottom would have a moderate degree of time lag and attenuation to approximate the expected behavior in a medium like the Tierra site. The differential displacement, ΔL, of the contaminant interface was on the order of 10 cm, corresponding to roughly 5% of the overall sample length.

To characterize the sands used in the pumping simulations, a number of preliminary experiments were performed. Porosity was determined by comparing bulk sample density with the density of SiO_2, and this was checked against the results of some gas flooding experiments. Porosity was on the order of 35% for all of the samples. Permeability was determined from measurements of pressure drop during steady flow of nitrogen, with the flow rate deduced from the long-term pressure drop in the nitrogen bottle. Permeability was around 30 Darcies versus 200 Darcies, for samples having mesh sizes of 60-100 versus 20.

Results of the first two tracer experiments are reported in Figure 10. The samples were identical. In one test, there was atmospheric pumping, while in the other there was none. So this is a comparison between molecular diffusion and mechanical dispersion. The two results are essentially equivalent, given the overall scatter of the data. In each test, the tracer arrived at the top of the column after about 30 hours, which compares fairly well with the following estimate, based on molecular diffusion

$$t \sim \frac{L^2}{\alpha} \sim 40 \text{ hrs}$$

Figure 9

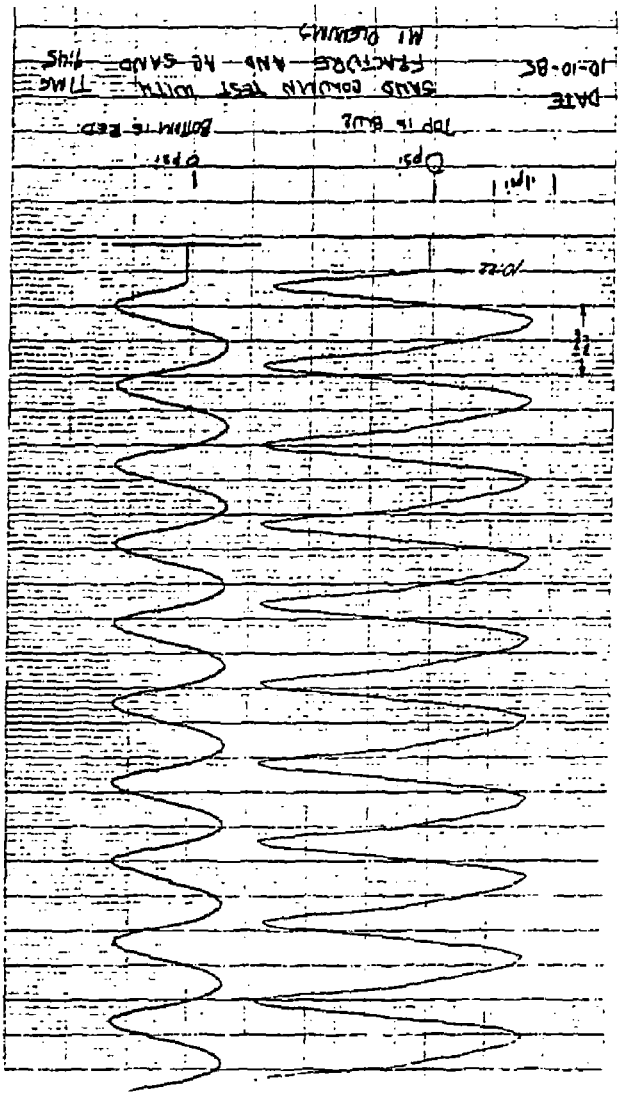

Figure 9. Typical pressure history at the top and bottom of the sand column during the laboratory experiments.

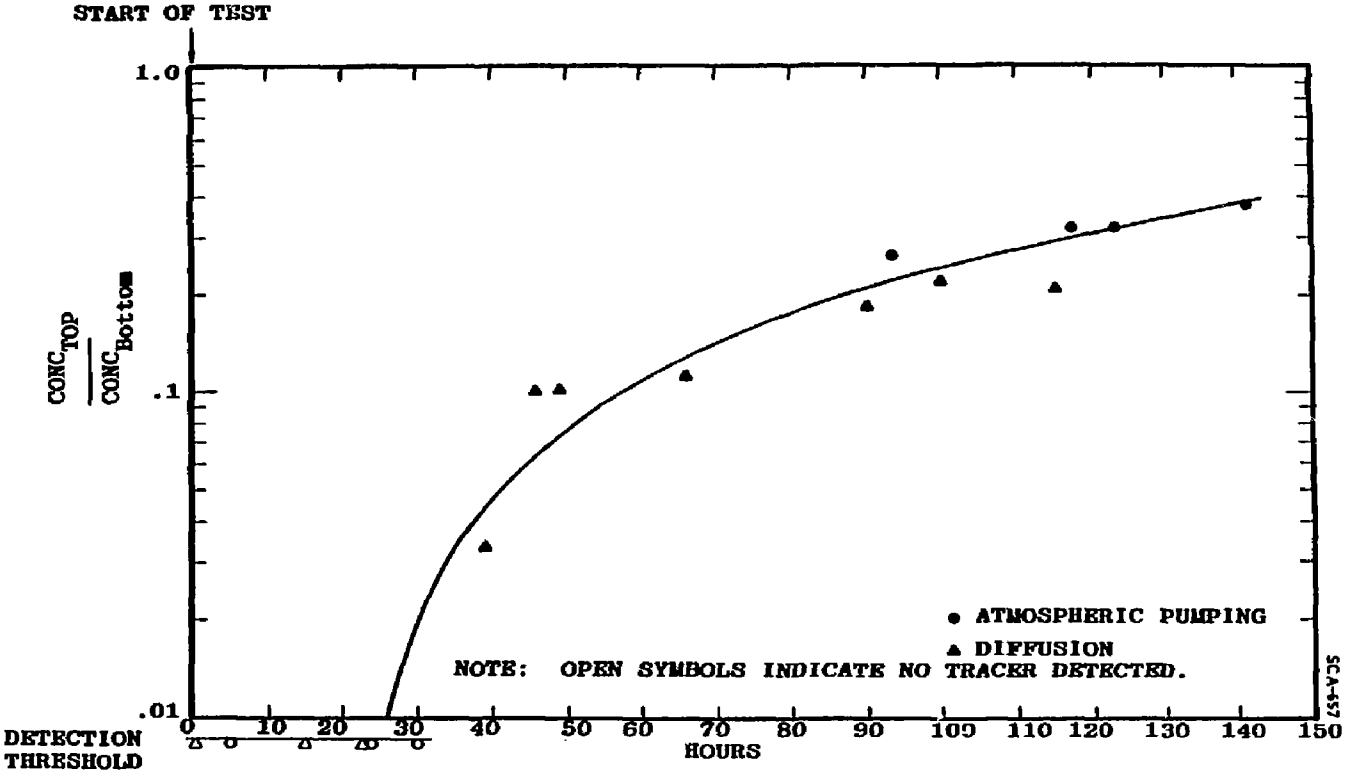

Figure 10. Comparison of atmospheric pumping and diffusion test results for 60-100 mesh glass spheres.

for L ~ 2 m and a molecular diffusion coefficient of 10^{-1} m^2/hr. No adjustment is made to account for the presence of sand grains since they are themselves impermeable, the grain size is fairly large, the bulk porosity is large, and the tortuosity is minor.

It was surprising, at first, to see that cyclical pumping did not enhance the dispersion and, hence, hasten the arrival of tracer gas. However, in homogeneous granular materials like sand, the dispersivity is generally on the order of 10^{-3} m or less. So with a pore velocity of about $u \sim \Delta L/\tau \sim 10$ cm/1 min. ~ 10 m/hr, the mechanical dispersion coefficient should be around

$$D_{mechanical} \sim 10^{-2}\ m^2/hr < D_{molecular} \sim 10^{-1}\ m^2/hr$$

suggesting that mechanical dispersion should not be noticeable in a unidirectional flow with this velocity. But, what about the ratchet or boot-strapping processes which could be active in our oscillatory experiments? Within those 30 hours of pumping, there were about 1000 cycles of motion, each with a 10 cm upstroke. This adds up to a total cumulative upward displacement of 100 meters for a demonic gas particle who always rides with the updraft and then holds his position during the downdraft.

The ratchet or boot-strap mechanism is not operative in a capillary tube or a homogeneous granular medium when the cross-channel diffusion time, $t = d^2/D$ is considerably less than the period of oscillation, because transverse molecular diffusion will then dissipate the horizontal concentration gradients which are essential to the mechanism. In our experiment with a grain size $d < 10^{-3}$ m, a molecular diffusion coefficient of $D \sim 10^{-1}$ m^2/hr, and a period of $\tau \sim .02$ hr,

$$\frac{t}{\tau} \sim 10^{-3} << 1$$

Thus, the theory predicts that there should be no ratcheting, and the experiment confirms that expectation - - which was quite a surprise to some of us skeptics.

The second pair of experiments shown schematically in Figure 11 was designed to illustrate the ratchet mechanism which we do expect to occur in fractured geologic media. To simulate the presence of a fracture or a high permeability path, we emplaced a 1 inch tube of coarse 200 Darcy sand along the centerline of the larger lucite tube, surrounding it with the finer 30 Darcy sand which was used in the previous experiments. In one case, the emplacement tube was left in position throughout the experiment, thus maintaining an impermeable barrier between the fracture and its permeable surroundings. In the other case, however, the tube was carefully removed during pouring and compaction of the annular sandpack, to allow free communication between the "fracture" and its surroundings.

The results of the two fracture-simulation experiments are shown in Figure 12. The arrival is clearly much earlier when the guard tube is removed, and the slope of the data is much steeper, suggesting a greater vertical flux. We believe that this enhancement is caused by the ratchet mechanisms pictured on the right side of Figure 6. Contaminated gas moves up the central column, and some of it travels outward into the surrounding annular sand pack, both by Darcian seepage and by molecular diffusion. Since the horizontal path length is now $d \sim 3$ cm, the transverse diffusion time of $t \sim d^2/D \sim 10^{-2}$ hr is comparable to the period of oscillation.

$$\frac{t}{\tau} \sim \frac{10^{-2}\text{hr}}{2 \times 10^{-2}\text{hr}} \sim 1$$

Thus, ratcheting should occur and it seems a likely explanation for the early arrival and enhanced contaminant flux observed in the simulated fracture experiment in which the guard tube was removed.

Comparison of the simulated fracture experiments with and without the guard tube helps to confirm the origin of the enhanced transport. The presence of the guard tube clearly delays the arrival and reduces the contaminant flux, even though the presence of the tube should tend to increase the upward displacement, ΔL, which occurs in the central column during each successive cycle. (The guard tube prevents lateral seepage from the central column into the surrounding annulus, which should increase the

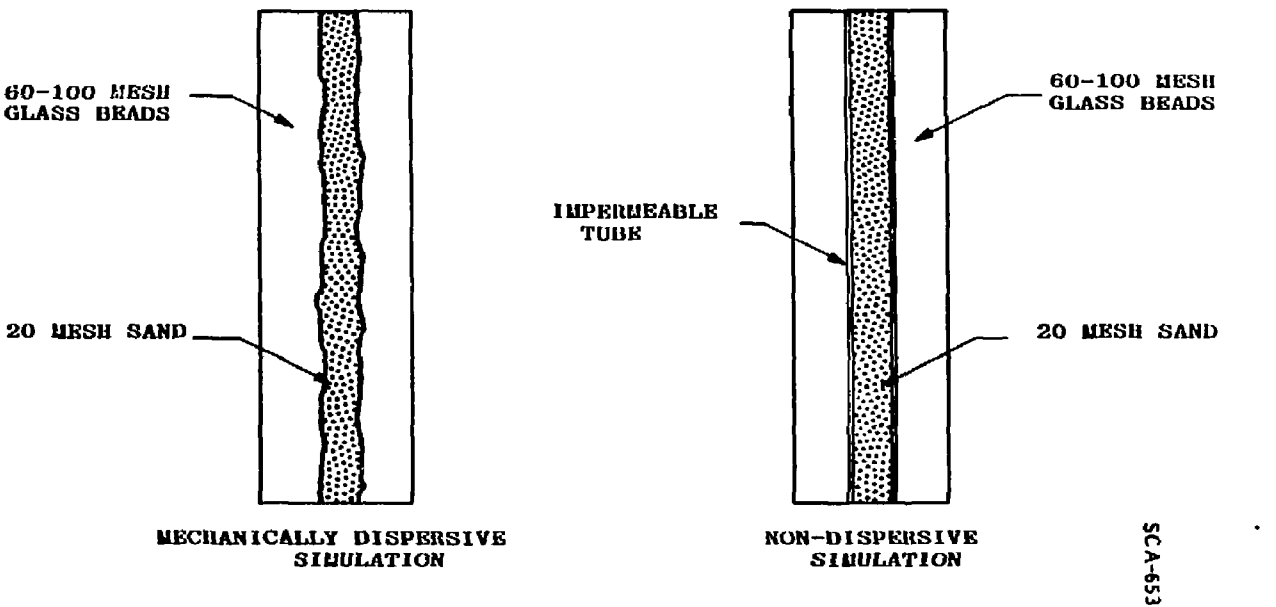

Figure 11. Interaction between a fracture and the surrounding porous medium is simulated by a high-permeability central column surrounded by an annulus of lower-permebility material. In some experiments, an impermeabile guard-tube was used to prevent crossflow between the "fracture" and its "porous" surrounding.

Figure 12

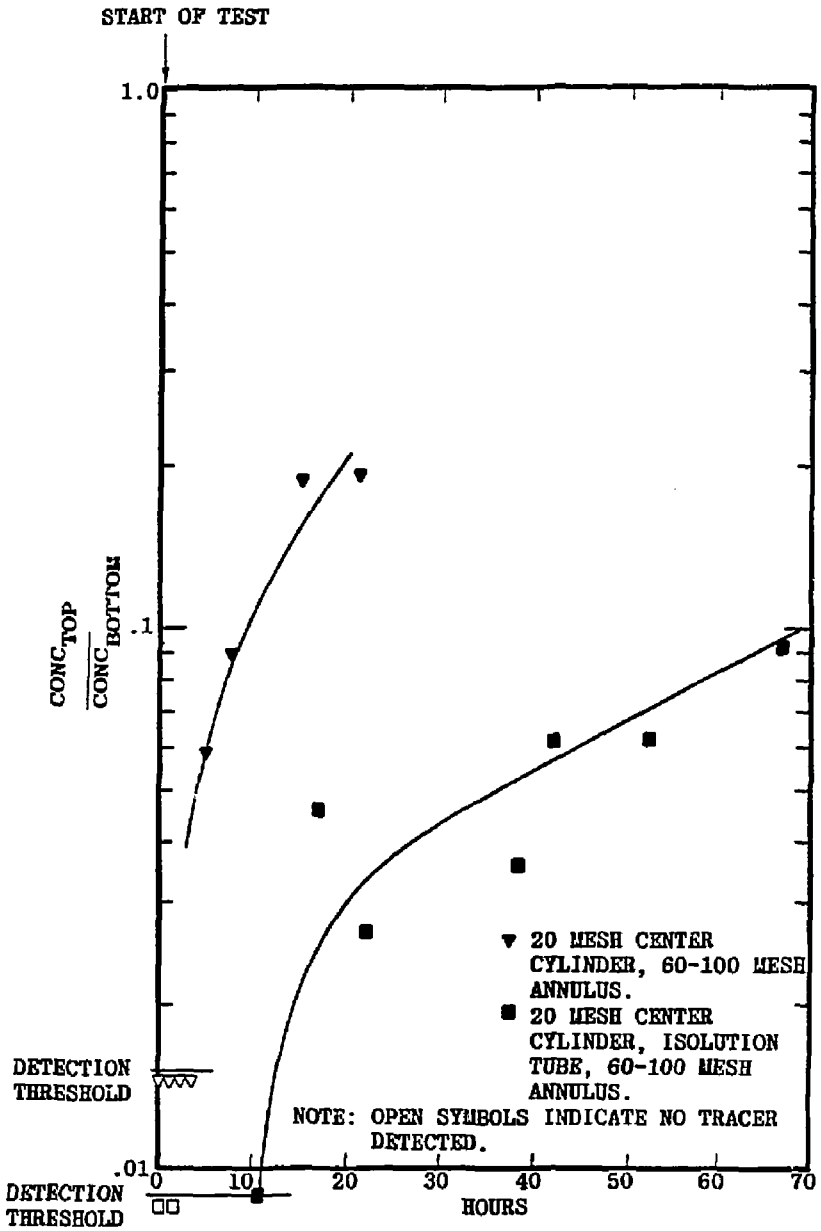

Figure 12. Comparison of results obtained with and without the guard-tube suggests that sideward communication between the "fracture" and its surroundings cause significant enhancement of the upward transport of contaminant.

"tidal displacement" ΔL.) Indeed, with the guard tube in place the contaminant has the opportunity to reach further toward the top on any given upstroke, but it cannot "hold" its position during a downstroke unless it is allowed access to a hiding place in the surrounding sand pack. The ratchet mechanism can only be effective if there is a transverse storage mechanism which has a relatively slow response time.

All of the experimental results are displayed in the composite of Figure 13. The fracture experiment with the tube absent clearly stands out from the others. The fracture experiment with the tube in place has a fairly quick arrival at the surface, but the late time flux (slope) is comparable to the first two experiments. These two observations (arrival and slope) together seem to suggest the following explanation: the arrival and the late time flux are both controlled by molecular diffusion; it's just that the larger differential displacement, $\Delta L \sim 1$ m, of the experiment with a central tube should reduce the path length for diffusion to at the surface.

In addition to the experiments already described, Figure 13 also includes a pumping test and a static diffusion test in which the entire tube was filled with coarse sand. The results are essentially equivalent to those discussed previously for the finer sand, confirming that the pore fluid diffusivity is not a controlling consideration whenever $\alpha\tau/L^2 >> 1$, as it is in these experiments and in the field applications of greatest concern.

The experiments outlined above strongly suggest that a ratchet-type dispersion mechanism may occur during atmospheric pumping of a fractured geologic medium owing to the interaction between vertical transport in the fractures and lateral transport within the porous matrix blocks. Such processes can be described by the so-called "double porosity" model discussed in the next section of this report.

4. DOUBLE POROSITY MODELING

Most geologic media contain natural fractures and, in the nuclear containment application of interest here, additional fractures are induced by the explosion and the subsequent cavity collapse. These fractures provide preferential paths for gas migration.

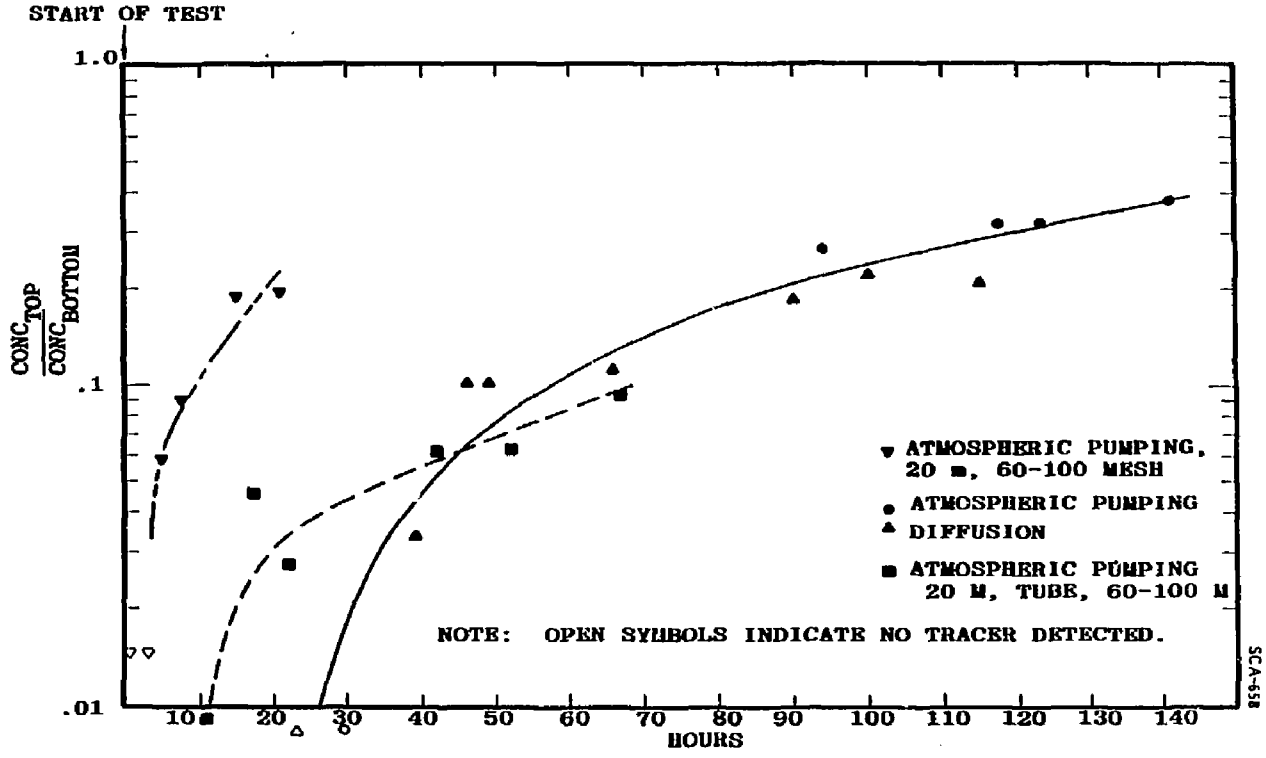

Figure 13. Composite of all results shows the contrast between the unguarded fracture simulations and all the other tests.

o formulate a mathematical model one might envision afracture pattern which divides the medium into slabs or blocks as illustrated in Figure 14. If the matrix blocks are entirely impermeable, it is a relatively simple matter to treat the fracture network as an equivalent permeable medium which is characterized by an effective porosity and permeability, ϕ_f and k_f. However, in most geologic media the matrix blocks have a porosity and permeability of their own (ϕ_m k_m), and it is important to take into account the exchange of fluid between the fracture network and the matrix blocks. The fluid exchange between the two porosities is particularly important in transient flow problems, like the one addressed here, because the matrix blocks contain most of the void volume (i.e., capacitance) of the system, even though the fractures serve as the primary flow channels (i.e., permeability).

Double porosity models allow a relatively complete description of a fractured permeable medium while still retaining a continuum viewpoint. In the simplest case having the slab geometry shown in Figure 14, it is appropriate to restrict attention to a single "unit cell" which consists of a single vertical fracture and the half-slab on either side: symmetry suggests that the vertical planes between cells (i.e., splitting the slabs in two) can be treated as impermeable no-flow boundaries. The behavior of this unit cell can be described by using one-dimensional channel flow equations to represent the flow in the fracture, coupled with a two-dimensional model of flow in the matrix blocks. Usually, the flow into the porous matrix can be treated as one-dimensional into the blocks. Given this simplification, one can easily extend the model from slabs to blocks, if one is willing to view a rectangular block as an equivalent sphere having pressure variation in the radial direction only. There are many variants of this double porosity theme, but the essential feature is the recognition of two different porosities, channels and blocks, with allowance made for exchange of fluid between the two. Of course, one can easily argue for triple porosity and more, in a complex geologic medium, but a two-level model should often provide a degree of sophistication which is commensurate with the data available to constrain it.

4.1 NUMERICAL IMPLEMENTATION OF DOUBLE POROSITY MODEL

A numerical model of fluid flow and contaminant transport in a double porosity medium has been formulated and implemented within the past several months as a part

figure 14

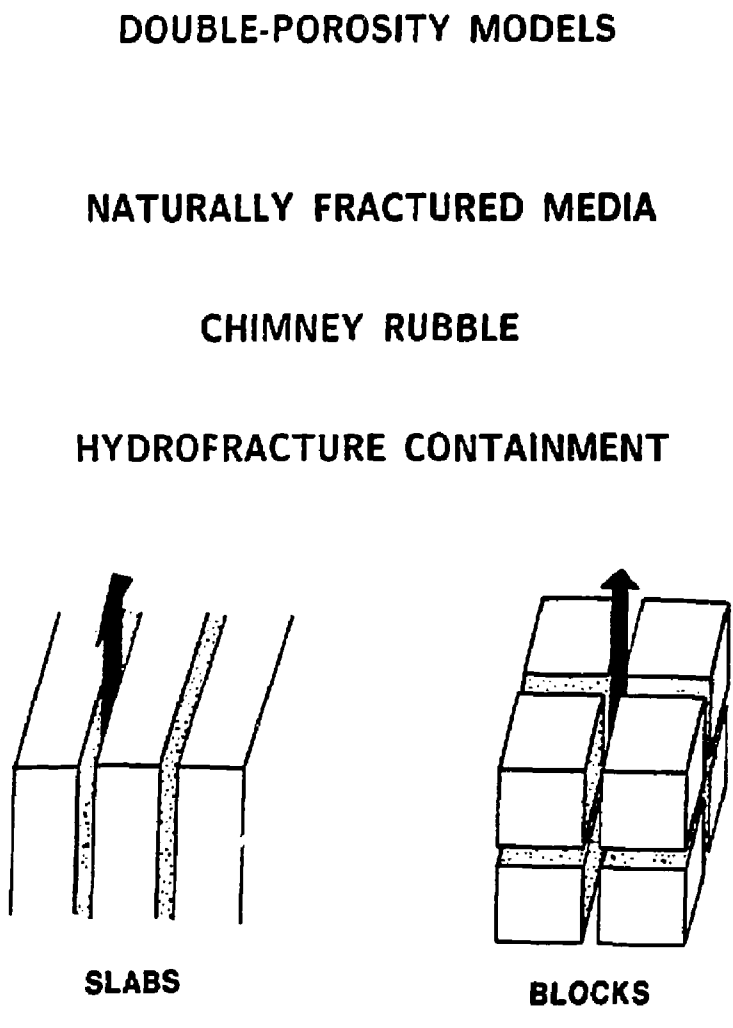

Figure 14. Double-porosity models which include fracture permeability as well as matrix-block permeability may be useful in describing many mechanisms of gas transport from a nuclear cavity toward the surface.

of this study concerning pumping. The coding draws heavily upon past work with Frank Morrison concerning transient fluid flow along isolated fractures in permeable media. Thus, the equations for fluid motion were already operative, and it was only necessary to add the diffusion-advection equations which describe the contaminant transport.

Numerical simulation of advective transport (i.e., contaminant carried along with the fluid flow) must be undertaken very cautiously, because the numerical scheme may inadvertently introduce an artificial diffusion mechanism which has a magnitude comparable to the actual physical mechanisms of diffusion and dispersion. This is particularly dangerous in the sort of study undertaken here where we hope to gain quantitative knowledge about complex physical processes for which we have no a priori order of magnitude estimates. Moreover, the cyclical character of the flow could permit a long term accumulation of numerical error which would not be so troublesome in the more common single-pass through-flow situations.

To guard against artificial dispersion, numerical testing was undertaken using two different methods, a standard upward difference technique as well as the FRAM (Filter Remedy and Methodology: M. Chapman, J. Comp. Phys., 1985) technique which seeks to minimize the numerical dispersion. Typical results are presented in Figure 15 which shows axial concentration profiles along a vertical sand column after completion of various numbers of cycles of oscillatory motion. Since there is no physical dispersion or diffusion in these solutions, the interface between contaminated and uncontaminated gas should always return to the same position at the end of each cycle, as it does in the far right frame which was calculated with the FRAM technique using 81 grid points along the column. The FRAM method introduces slightly more dispersion when the grid points are sparser, as seen by comparing the centerframe with the right hand frame in Figure 15, but in either of the FRAM calculations the numerical dispersion is relatively unimportant during the time period of the calculation. However, in the far left hand frame, which was calculated by a standard upwind difference technique, the numerical dispersion is so great as to spread the concentration profile all the way across the

Figure 15

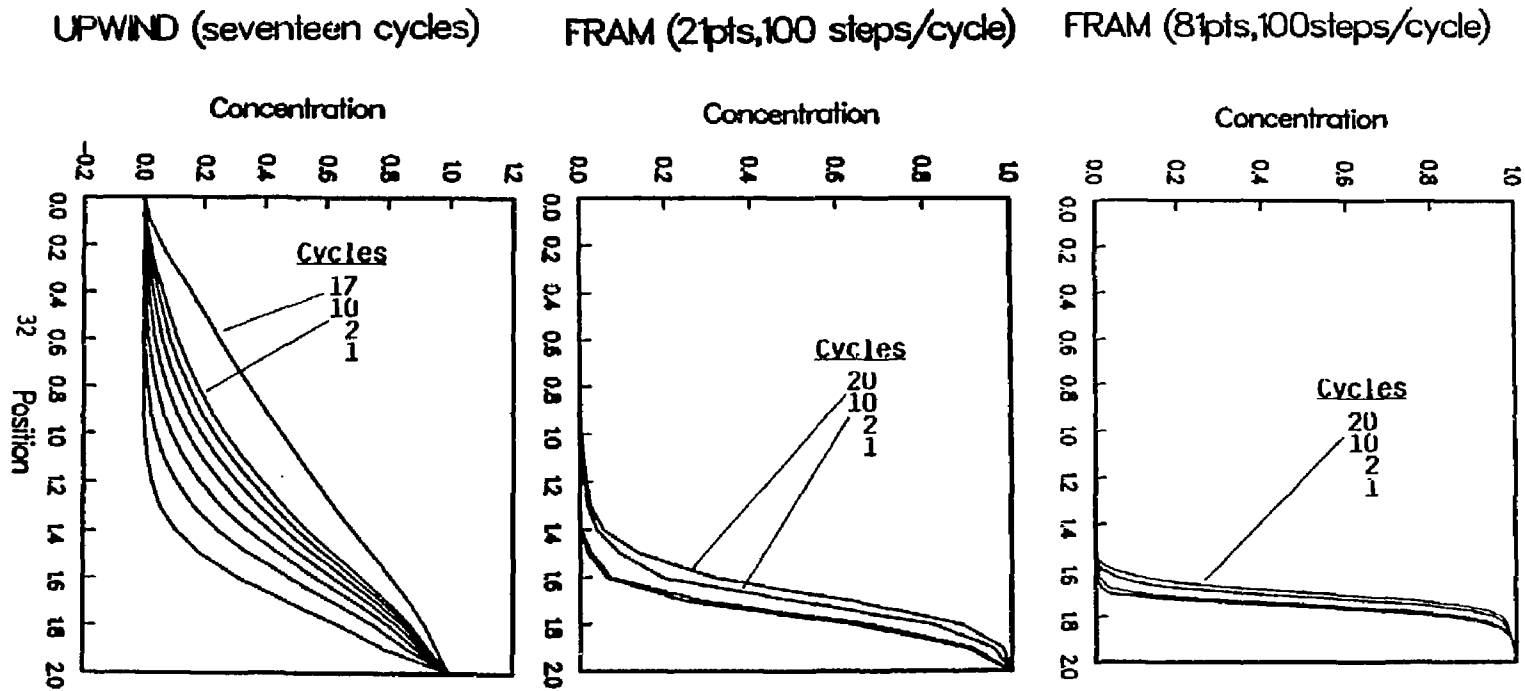

Figure 15. Computational experiments show that FRAM (Filtering Remedy and Methodology) is helpful in reducing spurious numerical dispersion, as compared with conventional upwind differencing techniques.

column during the 17 cycles of oscillatory motion. Thus we adopted the FRAM techniques for use in our double porosity modeling, and we will take care to insure that artificial dispersion is always considerably less than the physical dispersive mechanisms which we seek to model in subsequent applications.

4.2 HOMOGENEOUS EXAMPLE

Although the double porosity model generally applies to a fractured porous medium, it can be easily degenerated to the case of a homogeneous porous medium which contains no fractures. This serves as a test case for the numerics and as a baseline case for comparison with fractured media and double-porosity media.

The example problem in Figure 16 is a crude approximation to the posttest configuration of Tierra. A cavity-sized chimney void is connected to the surface through a 200 meter column of overburden material having a permeability of 350 Darcies and a porosity of 0.1. These parameters correspond to a pore fluid diffusivity of $\alpha = kP_o/\mu\phi$ ~ 60,000 m^2/hr, comparable to the preshot values inferred by John Hansen from atmospheric pumping data.

The pressure at the surface of the medium, labeled P_{top} in Figure 16 is prescribed as a sine wave with a period of 100 hours and a peak-to-peak amplitude of 1/30 atm, centered about 1 atm. the calculated chimney pressure, labeled P_{bottom} in Figure 16 closely tracks the surface pressure, in a fashion which somewhat resembles the observed preshot behavior of the Tierra emplacement hole.

Since the transit time, t, for a pressure wave to traverse the medium is considerably less than the period, τ, of pressure oscillation,

$$\frac{t}{\tau} = \frac{L^2/\alpha}{\tau} \sim \frac{1}{100} \quad .$$

the flow in the column is essentially quasisteady at all times. So the phase lag and the attenuation of the pressure are controlled by the steady-flow fluid conductance (volumetric flow rate, Q, driven by a given pressure drop, ΔP)

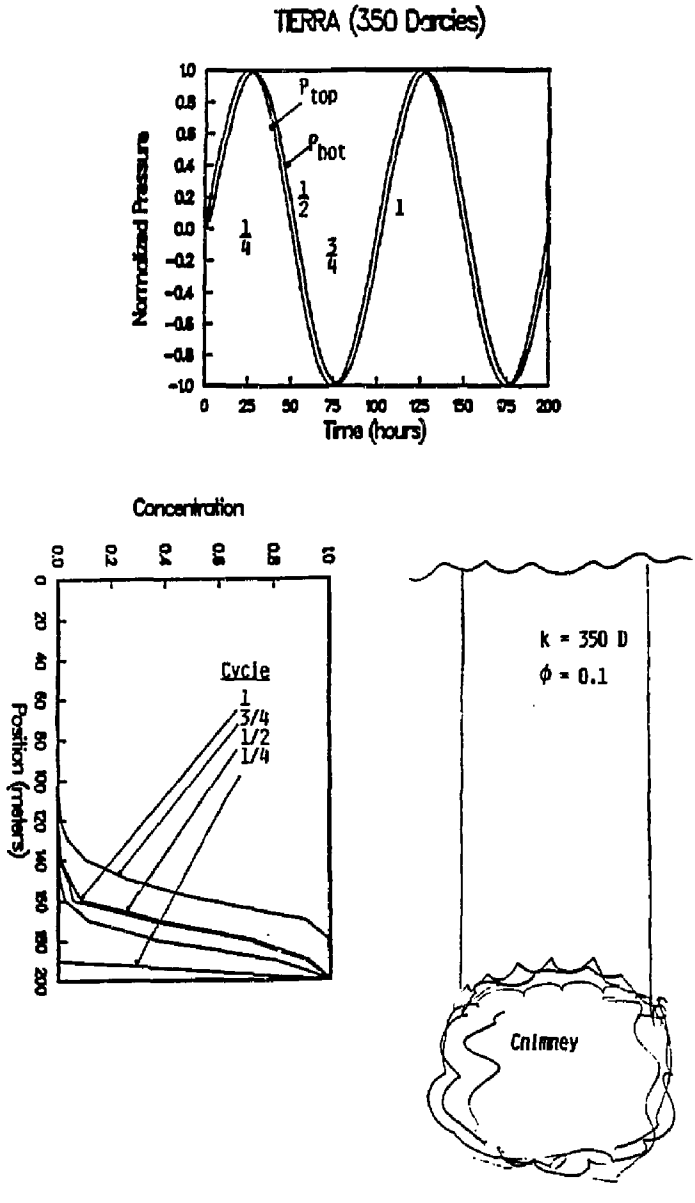

Figure 16. Pressure histories and corresponding contaminant profile for a homogenous medium (350 D, 0.1) above a collapsed nuclear cavity. During first atmospheric low, contaminant only moves upward by 50 m or so.

$$\frac{Q}{\Delta P} = \frac{uA}{\Delta P} = \frac{kA}{\mu L}$$

and by the capacitance or volume of the chimney void, $V_c \sim 10^6$ m^3, which is a few times greater than the pore volume in the column above, $V_p \sim \phi A_{cc} L \sim 2x10^5$ m^3.

Profiles of contaminant concentration versus position at various instants in time are also included in Figure 16. Only 1 full cycle of time is shown, but all subsequent cycles would be identically the same, because this calculation has no molecular diffusion nor mechanical dispersion. For the first 1/4 cycle, the surface pressure is rising, so the flow is downward and there is no upward transport of contaminant. Over the next 1/2 cycle the pressure is falling and the flow is upward, so the contaminant interface advances upward by a differential displacement

$$\Delta L \sim \frac{V_o}{\phi A_{cc}} \frac{\Delta P}{P_o} \sim 35 \text{ m}$$

as seen for the profile labeled 3/4 cycle. The front then begins to recede again as the pressure rises into the next cycle.

The primary purpose of this calculation is to reinforce the ideas introduced previously in Section 2 concerning the roles of buffer volume and diffusivity. It is also useful for comparison with fracture-dominated calculations in the next example problem.

4.3 FRACTURE-DOMINATED EXAMPLE

In contrast to the previous example of a homogeneous porous medium with a uniformly distributed porosity of 10%, let us now consider the opposite extreme of a fracture-dominated medium in which the only accessible porosity is that of the fracture network itself. Further suppose that the fractures are separated by slabs with a breadth of B = 1.0 m, and that each fracture has an aperture of w = 1.7 mm, such that the steady flow fluid conductance

$$\frac{Q}{\Delta P} \approx \frac{UA}{\Delta P}\left(\frac{w}{B}\right) = \frac{w^2}{12}\frac{A}{\mu L}\frac{w}{B}$$

is numerically the same as it was in the preceding example. Then, for the same cavity volume beneath the column, we calculate a pressure variation in the chimney which is essentially the same as before. The pore fluid diffusivity is now much greater than before, and the wave transit time is much smaller than it was, but this has very little effect on the chimney pressure response, since the wave transit time is, in both cases, small compared to the period of oscillation.

The primary difference between the homogeneous and fractured cases is that the porosity of the fractured medium is only $\phi_f \sim w/B \sim 0.0017$ compared to $\phi_m \sim 0.1$ for the homogeneous case. Thus, the buffer volume within the fractures is now

$$V_{fractures} \sim \phi_f A_{cc} L \sim \frac{1}{100} V_{cavity}$$

which is too small to accommodate the differential expansion of the cavity gas

$$\Delta V_{cavity\ gas} \sim \frac{\Delta P}{P_o} \times V_{cavity} \sim \frac{1}{30} V_{cavity}$$

So, the difference will be vented to the atmosphere

$$\Delta V_{vent} \sim \Delta V_{cavity\ gas} - V_f \sim \frac{2}{100} V_{cavity}$$

This venting behavior is also apparent in the concentration profiles of Figure 17 which indicate that the fractures are full of contaminated gas and venting during lows, but full of fresh gas during highs.

Thus far in these comparative calculations for homogeneous versus fractured geologic media we have exercised either a matrix porosity or a fracture porosity, without allowing any interaction between the two. In the next section we consider the coupled case where the two porosities are interconnected.

Figure 17

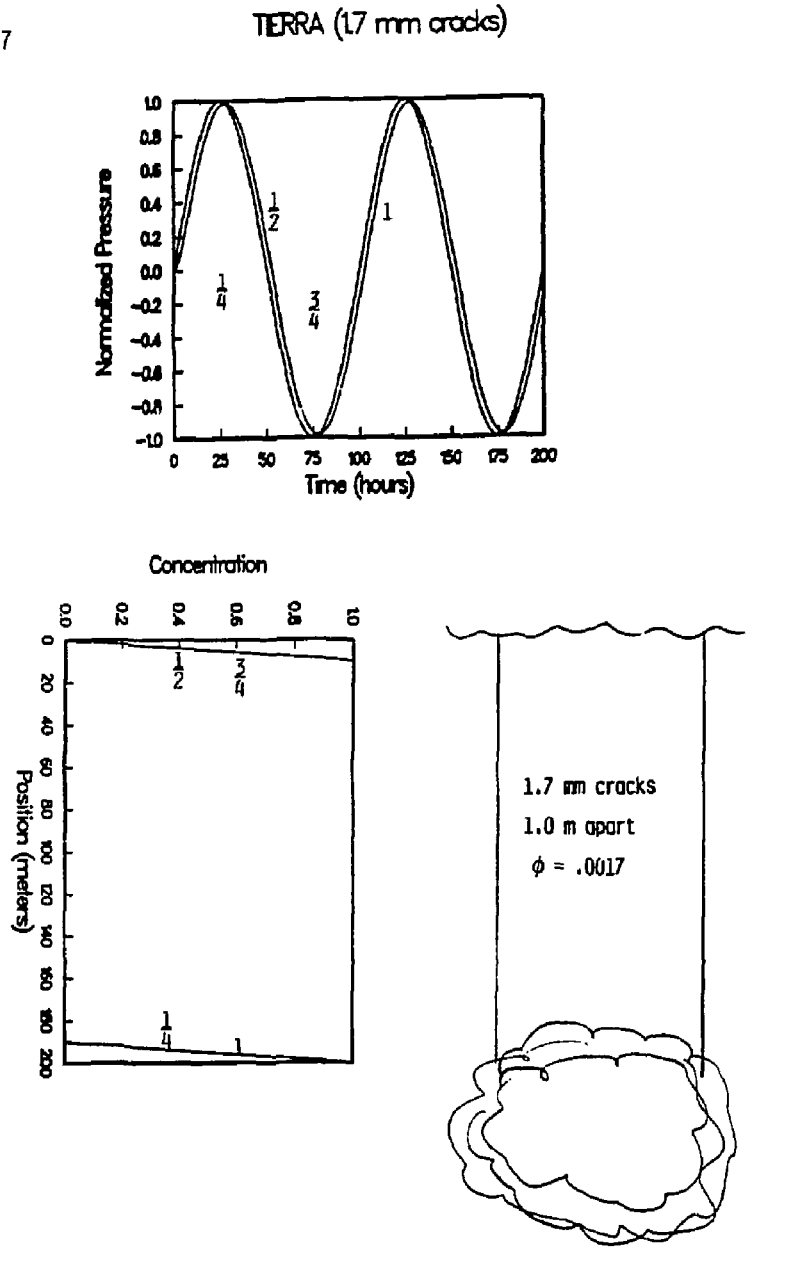

Figure 17. *Pressure histories and corresponding contaminant profile for a fractured porous medium above a collapsed nuclear cavity. Pressure signature is the same as for homogenous medium in Figure 16, but contaminant now reaches surface during first atmospheric low.*

4.4 DOUBLE POROSITY EXAMPLE

Some preliminary results for pressure wave propagation in a double porosity medium are now available, but we have not yet completed the coding required for a two-dimensional treatment of the diffusion-advection equations which describe the transport in the matrix blocks. Even so, it is possible to make some qualitative observations on the character of the pressure transients and the associated transport for the double porosity case.

First, the previous calculations have demonstrated that the transient pressure response of a nuclear chimney or an emplacement hole may be controlled by the steady flow conductance of the surrounding medium, particularly in the threatful cases where the diffusivity is high. In fractured geologic media it is generally true that the steady flow characteristics are primarily determined by the permeability of the fracture network, even in cases where there is a secondary matrix-block porosity. Thus, this sort of quasisteady pressure response data should provide a good indication of fracture network permeability but may furnish little information concerning matrix block permeability or the porosity available within either the fracture network or the porous blocks. In this context it is reiterated that the presence of a large buffer porosity is often a key consideration in the surface arrival of contaminant.

Secondly, even if a pressure measurement does succeed in measuring the "diffusivity" of a double porosity medium (i.e., the transit time of a pressure wave or associated quantity), it may be very difficult to unfold the meaning of this measurement in terms of the fundamental transport properties (e.g., porosities or permeabilities of the fractures or the matrix). This is because the propagation of the pressure wave is controlled by different matrix properties within different regimes of time and length of run, as illustrated by the example calculation of Figure 18. The symbols in Figure 18 represent numerically calculated penetration distance versus time for propagation of a step-induced pressure wave in a double porosity medium. At very early times the pressure disturbance moves along the fractures just as

Figure 18

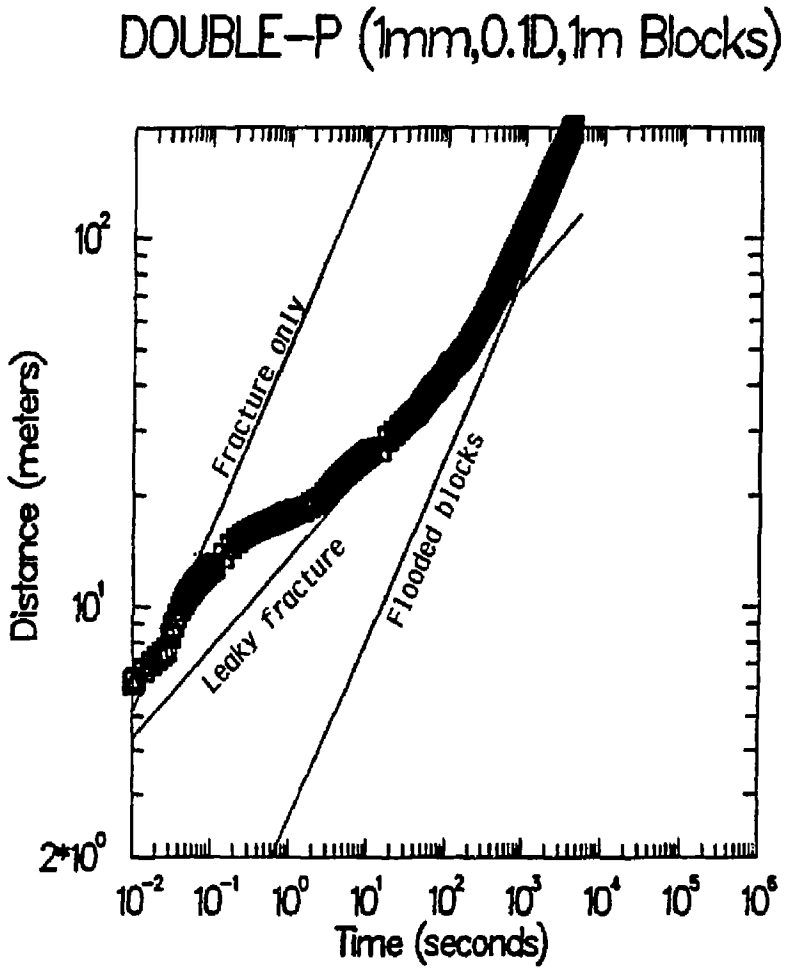

Figure 18. Three different regimes of fracture/matrix interaction occur during the propagation of a pressure wave in a double-porosity medium.

though the surrounding matrix blocks wereimpermeable. Within this regime the penetration distance increases like the square root of time and it depends only upon the aperture of the fractures. At intermediate times, most of the fluid flowing into the fracture is lost to the surrounding blocks. Within this regime the propagation distance grows like the fourth root of time and it depends upon the aperture of the fractures as well as the permeability and porosity of the surrounding matrix blocks. Finally, at very late times, the growth returns to the square root of time; within this regime the double porosity composite behaves as though it has the permeability of the fracture network but the total porosity or capacitance associated with the fractures and the blocks. Thus, a relatively complete set of data is required to discern the various parameters.

Thirdly, a measurement of pressure arrival or "diffusivity" may furnish very little indication of the associated contaminant arrival. This was illustrated previously for single-porosity systems under quasi-steady pumping (i.e., $L^2/\alpha << \tau$), but in the double-porosity case, there is a more subtle difficulty which is illustrated schematically in Figure 19.

1. In a single-porosity medium, either homogeneous or fractured, there is no opportunity for fluid to "pass up" fluid, so the contaminated gas can reach the surface only by displacing all of the gas above it (neglecting the Taylor dispersion explained previously). The propagating wave induces a particle velocity which is smaller than the wave velocity by a factor of roughly $\Delta P/P_o << 1$. Since the contaminant travels with the gas particles the contaminant interface lags behind the pressure disturbance by a factor of $\Delta P/P_o << 1$.

2. In a double-porosity medium, however, the fluid in the fractures clearly "passes up" the matrix fluid during an upflow phase, so the fracture fluid can reach the surface without displacing the matrix fluid. Thus, as indicated in Figure 19, the contaminant interface may be nearly coincident with the leading edge of a pressure disturbance in a double porosity medium.

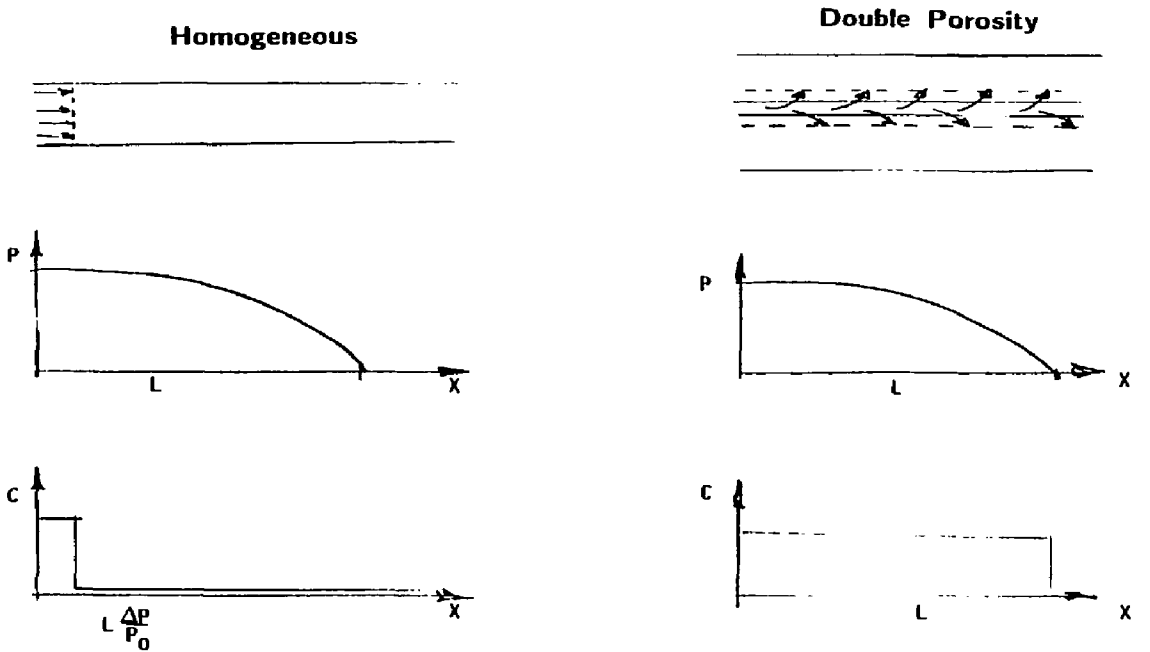

Figure 19. Contaminant transport and arrival may be very different in a double-porosity vs. homogeneous media, even though the pressure-wave arrival is comparable.

Reconsider now the question of "buffer" porosity between the contaminated gas and the earth's surface. In many cases the total porosity of the overburden is more than sufficient to accommodate the expansion of the cavity gas during atmospheric pumping, but the partial porosity of the fracture network is far too small. Thus, it is necessary to ask what fraction of the matrix-block porosity is actually accessible or useful as a buffer volume. This question is very difficult to answer on the basis of pressure measurements alone.

The buffering effectiveness or efficiency of the overburden porosity is closely related to the oilfield concept of "displacement efficiency". During water flooding operations, water is pumped into injection wells with the intent of driving oil toward the production wells. To accomplish this purpose,the water bank must shove the oil ahead or displace it. An efficient displacement might not be achieved in a highly fractured medium if the water were simply to flow from the injection well to the producer well, bypassing the oil within the matrix blocks. In our containment application, we would similarly prefer an efficient displacement of fresh gas by contaminated gas during atmospheric pumping, since this would allow more of the total porosity to serve as a buffer volume for expansion of the contaminated gas.

5. MULTIDIMENSIONAL EFFECTS

All of the analysis and experiments described in the preceding sections are based on one-dimensional models of vertical transport, as illustrated in Figures 1 and 2. Consideration was given to the multidimensional effects which occur on the scales of pore size, fracture aperture, and matrix blocks. These effects were accounted for in a quasi-one-dimensional fashion by the introduction of a dispersion coefficient and a double-porosity formulation. However, the primary flow direction has, thus far, been upward through the chimney. There has been no explicit mention of the horizontal flow between the chimney and its surroundings.

Depending upon the difference in transport properties between the chimney and its surroundings, the horizontal transport could either aggravate or mitigate the upward transport of radioactive gases.

1. If the pressure in the chimney "leads" the pressure in the surroundings (at any given elevation), fresh air will be drawn into the chimney during a falling barometer, which would tend to aggravate the upward transport of gas through the chimney.

2. If the chimney "lags" the surroundings, radioactive gas will be drawn from the chimney into the surroundings during a falling barometer, which should tend to mitigate the vertical transport.

Whether or not the chimney leads or lags would depend upon the relative diffusivity of chimney and surroundings, if each of the "columns" could be viewed as a homogeneous medium. This sort of comparison would suggest a "leading" chimney, since the explosion and collapse should probably increase the permeability. However, bulking processes or partial collapse would tend to increase the void volume in the chimney and there might be an increase in the connectivity between matrix blocks and fracture networks, which should increase the apparent porosity and, hence, suggest a "lagging" chimney.

Postshot monitoring of pressure in the chimney and the surroundings would provide some insights as to whether or not the chimney is leading or lagging during atmospheric pumping.

One-dimensional modeling of dispersion effects and double-porosity interactions is viewed as a first step toward understanding these processes in their simplest context. The same concepts, numerical techniques, and property data can then be applied to the more complex multidimensional problem.

Laboratory experiments could be easily conducted to demonstrate the effects of a leading or lagging chimney. In fact, the sand column experiments with a high-permeability center were similar in concept and interpretation. The dispersion mechanism pictured at the far right of Figure 6 can operate either on the microlevel of fractures and blocks or the macrolevel of chimney and surroundings.

6. SUMMARY

Radioactive gases might be drawn upward to the earth's surface as a result of atmospheric pressure variations. Depending upon the properties of the medium and the configuration of the chimney, several different situations might occur.

1. If the pore fluid diffusivity of the medium is sufficiently small and the radioactive gases sufficiently deep that

$$\frac{L^2}{\alpha} \gg \tau$$

(where τ is the period of atmospheric pumping), then the pressure disturbance would hardly be felt at the contaminant depth, and the upward gas motion would be negligible. This situation would occur in media having a large scale bulk permeability of 1 Darcy or less, provided no significant fractures were present.

2. A large diffusivity need not be threatful, provided that the accessible buffer porosity between the contaminated gas and the surface is sufficiently large to accommodate the expansion of the cavity gas which occurs during atmospheric lows.

3. Even though the buffer porosity may be sufficient to accommodate the differential expansion which occurs on any one cycle of pumping, successive cycles may still transport contaminated gas to the surface as a result of the ratchet-like dispersion mechanisms which can occur in oscillatory flows.

All three of the issues noted above are critically dependent upon the non-homogeneity of the medium and in particular the role played by the natural or explosively induced fractures. The presence of fractures or nonhomogeneities will influence all three of the mechanisms noted above as well as the associated properties or attributes listed below.

1. Pore fluid diffusivity

2. Accessible porosity or displacement efficiency

3. Dispersivity

Each reflects the presence of nonhomogeneities, but only in ways which are relatively difficult to apply in an unambiguous way.

From a containment viewpoint the worst situation is one in which there are a few major fractures surrounded by a relatively impermeable material. The diffusivity would then be very rapid along the fractures, but very slow on the average. The accessible buffer volume would be negligible, and the dispersion would be very large. Yet, such a situation might be difficult to diagnose beforehand, because of the following considerations.

1. The most important fractures might be induced by the explosion or the collapse.

2. Borehole measurements in the undisturbed media might "miss" the fractures, particularly if they are sparse.

3. Atmospheric pumping data from the emplacement hole provides a good indication of the connectivity between the hole and the surface, but it may be strongly influenced by near- surface layers and it is difficult to distinguish between homogeneous media and fracture-dominated media.

Notwithstanding these difficulties, the acquisition and analysis of such data should lead to a better understanding of the physical processes, a better characterization of the emplacement media, and ultimately, a better estimation of the contaminant transport to the surface. In particular, the combination of pressure response data with tracer arrival data should be helpful in characterizing the degree of nonhomogeneity which appears to be at the heart of the issue.